Proc. of the Third Intl. Conf. on Advances in Civil, Structural and Construction Engineering - CSCE 2015

ISBN: 978-1-63248-079-8 doi: 10.15224/ 978-1-63248-079-8-50

Moment-curvature relation of Reinforced Concrete T-beam sections - Numerical and Experimental studies

Swapnil Joshi, Shinto Paul, Bijily Balakrishnan, Devdas Menon

***Abstract*— A simple algorithm is proposed to develop a nonlinear moment-curvature relation for Reinforced Concrete (RC) T-beam sections using nonlinear material models. The flange in the beam adds to the complexity of analysis compared to rectangular beam sections. This algorithm has been validated by laboratory testing of simply supported flanged beam specimens, subjected to two-point loading. The load-deflection data obtained from the experiments is converted to a moment-curvature relation for the section applying simple bending theory. The results predicted numerically by the proposed algorithm are found to be in good agreement with the experimental data. The algorithm developed can be used to generate the load-deflection curve of an RC T-beam subject to any given loading.**

***Keywords*— reinforced concrete, T-beam, moment-curvature , nonlinear analysis**

I. Introduction

Flexural behavior of a reinforced concrete section can be studied with the knowledge of its moment-curvature relation. It is an important tool in generating moment field in a linear or nonlinear analysis as well as in predicting the complete nonlinear load-deflection behavior of RC flexural members. This relation is nonlinear mainly due to concrete cracking and steel yielding, which makes the analysis fairly complicated. Therefore for simplicity, it is sometimes idealized as bilinear or trilinear [1]. However to predict the response more accurately, it becomes necessary to incorporate nonlinear effects accounting for flexural cracking that capture the progressive flexural degradation under incremental loading.

Various models are available in the literature for predicting the moment-curvature relation of RC sections. Some of these models are simple but predicts the behavior up to service loads only. To predict the curvatures and deflections beyond service loads, Bažant and Oh [2], Carreira and Chu [3-4], and Prakhya and Morley [5] proposed nonlinear stress-strain models. In the present study, how a moment-curvature relation can be developed for reinforced concrete T-beam sections is shown. Such sections are commonly encountered in continuous slab systems supported on beams as well as in bridge deck systems.

Swapnil Joshi, Graduate student

Shinto Paul, Bijily Balkrishnan, Doctoral Student

Devdas Menon, Professor

Indian Institute of Technology Madras, India

A portion of continuous slab integrally connected to the beam serves as flange and the supporting beam as web. The flexural capacity of such sections can be enhanced when the flanges are in compression. The web helps in resisting shear stresses.

The moment-curvature relation is obtained by carrying out sectional analysis of RC T-beam section. In this analysis, different cases are considered depending on the position of the neutral axis [6]. Testing of three T-beams has been carried out in the laboratory. These beams are loaded symmetrically at two points to simulate pure flexure. Load-deflection data obtained from these tests is used to generate moment-curvature relation using theory of simple bending. The results generated by numerical algorithm are validated with these experimental results. The behavior of the beams is studied for variation in depth of flange and tensile reinforcement. The nonlinear sectional analysis for these RC T-beams is explained in the next section.

II. Sectional analysis of RC T-beam

Nonlinear sectional analysis of RC T-beam incorporates material models to account for the material nonlinearities due to cracking of concrete, yielding of steel and strain softening. Euler-Bernoulli hypothesis (plane sections normal to the beam axis before bending remain plane and normal after bending) is assumed to hold good throughout the analysis. Also the overall bond slip is assumed to be zero.

A. *Material Models*

Stress-strain behavior for concrete in uniaxial compression which takes into account compression strain-softening [7] as shown in Fig. 1 (a) is implemented in proposed algorithm.

$$\sigma_c = \frac{E_c \varepsilon_c}{1+\left(\frac{E_c \varepsilon_{c_0}}{f_c}-2\right)\left(\frac{\varepsilon_c}{\varepsilon_{c_0}}\right)+\left(\frac{\varepsilon_c}{\varepsilon_{c_0}}\right)^2} \quad (1)$$

where E_c is the short term elastic modulus of concrete in N/mm^2, f_c is the peak stress in compression in N/mm^{2}and ε_{c0} is the strain at peak compressive stress and assigned as

$$\varepsilon_{c_0} = \frac{2 f_c}{E_c} \quad (2)$$

The expression for ε_{c0} is the smallest value which gives a realistic stress-strain curve [8]. The value of ε_{c0} has an approximate value of 0.002. For concrete in tension an idealized bilinear stress-strain curve is used as shown in Fig. 1(b) and tensile stress (f_t) is formulated as below.

$$\text{For } \varepsilon_t \le \varepsilon_{tp};\ f_t = E_c \varepsilon_t \quad (3)$$

Proc. of the Third Intl. Conf. on Advances in Civil, Structural and Construction Engineering - CSCE 2015

ISBN: 978-1-63248-079-8 doi: 10.15224/ 978-1-63248-079-8-50

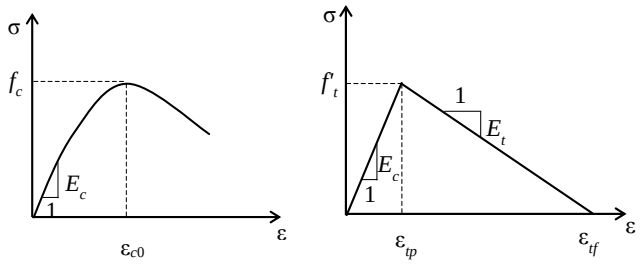

Figure 1(a) Stress-strain curve for concrete in compression (b) tension

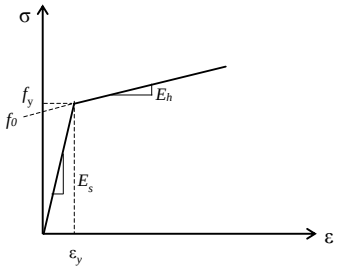

Figure 2 Stress-strain curve for steel with strain-hardening

For $\varepsilon_{tp} < \varepsilon_t < \varepsilon_{tf}$; $f_t = f_t^{'} + E_t\left(\varepsilon_t - \varepsilon_{tp}\right)$ (4)

For $\varepsilon_t > \varepsilon_{tf}$; $f_t = 0$ (5)

where f_t and ε_t is uniaxial stress and strain of concrete in tension respectively, ε_{tp} is the strain at peak tensile stress, ε_{tf} is the final tensile strain when the tensile stress reduces to zero, $f_t^{'}$ is the direct tensile strength in N/mm^2 and E_t is tangent strain-softening modulus and is given by[2]

$$E_t = \frac{-70E_c}{57 + f_t^{'}} \quad (6)$$

where E_c, $f_t^{'}$ and E_t are in psi (1 psi =6895 N/m^2)

Direct tensile strength $f_t^{'}$ is taken as [9]

$$f_t^{'} = 0.34\sqrt{f_c} \quad (7)$$

The expressions for the strain at peak stress (ε_{tp}) and for the final strain (ε_{tf}) when stress reduces to zero can be simply derived from the Fig. 1 (b) as

$$\varepsilon_{tp} = \frac{f_t^{'}}{E_c} \quad (8)$$

$$\varepsilon_{tf} = \frac{f_t^{'}}{E_c} + \frac{f_t^{'}}{E_t} \quad (9)$$

For steel, an idealized bilinear stress-strain curve with strain hardening region, has been proposed by Belarbi and Hsu [10]. This model is adopted for present study as shown in Fig. 2 and stress in steel (f_s) is expressed as

For $\varepsilon_s \le \varepsilon_y$; $f_s = E_s\varepsilon_s$ (10)

For $\varepsilon_s > \varepsilon_y$; $f_s = f_0 + E_h\varepsilon_s$ (11)

where f_s is the stress in steel at the strain of ε_s and, ε_y is the yield strain, E_s is the elastic modulus of steel in N/mm^2 and E_h is the modulus of steel in the strain-hardening region.

B. *Generation of moment-curvature relationship*

A more realistic approach that account for the material nonlinearities due to concrete and steel is adopted in the present study. The analysis considers two cases, neutral axis inside the flange region, and neutral axis outside flange. Nonlinear stress-strain curve for concrete in compression mentioned above has been adopted in the algorithm. Strain-hardening in steel provides nonlinear behavior due to yielding of steel. All nonlinearities together make the analysis more accurate and in turn provides a perfect input for the nonlinear analysis of the structure.

Variation of strains and stresses for a typical RC T-beam section is shown in Fig. 3. Area of reinforcement in tension and compression are A_{st} and A_{sc} respectively. Strains in the reinforcement in tension and compression are ε_{st} and ε_{sc} and the corresponding stresses are f_{st} and f_{sc}.

The force resultants for the reinforcement in tension (S_t) and in compression (S_c) are given by equation

$$S_t = f_{st}A_{st} \quad (12)$$

$$S_c = f_{sc}A_{sc} \quad (13)$$

With the known value of strain at the extreme compression fiber ε_{cm} and the depth of neutral axis kd (d is effective depth of the beam), strains at the level of reinforcement (neutral axial above cover) can be calculated using similar triangles as follows

$$\varepsilon_{st} = \varepsilon_{cm}\frac{d - kd}{kd} \quad (14)$$

$$\varepsilon_{sc} = \varepsilon_{cm}\frac{kd - d^{'}}{kd} \quad (15)$$

A. Neutral axis inside the flange $\left(kd \le D_f\right)$

When the neutral axis lies inside the flange, a small portion

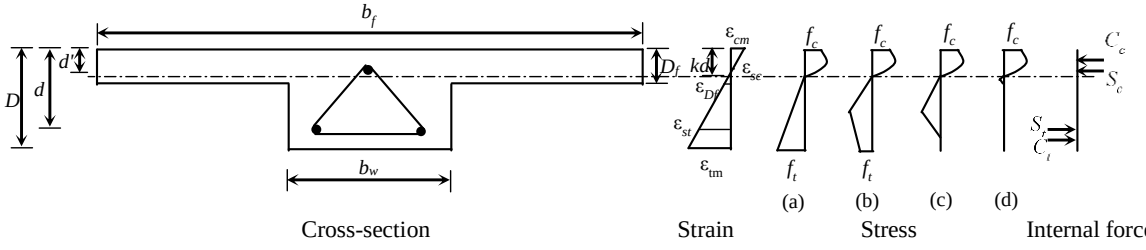

Figure 3 Cross-section of T-beam showing variation of strains and stresses for neutral axis inside the flange

Proc. of the Third Intl. Conf. on Advances in Civil, Structural and Construction Engineering - CSCE 2015

ISBN: 978-1-63248-079-8 doi: 10.15224/ 978-1-63248-079-8-50

of the flange and the web carries tension along with the reinforcement. Further we need to consider various cases depending upon the lines of tensile stress peaks and of the points where the tensile stress reduces to zero, relative to the bottom of the flange as shown in Fig. 3.

Various cases depending on the values of ε_{tp} and ε_{tf} are considered for the analysis. These are listed below.

a) $\varepsilon_{tm} \le \varepsilon_{tp}$

b) $\varepsilon_{tp} < \varepsilon_{tm} < \varepsilon_{tf}$

i) $\varepsilon_{D_f} \le \varepsilon_{tp}$

ii) $\varepsilon_{D_f} > \varepsilon_{tp}$

c) $\varepsilon_{tm} \ge \varepsilon_{tf}$

i) $\varepsilon_{D_f} \le \varepsilon_{tf}$

ii) $\varepsilon_{tp} < \varepsilon_{D_f} < \varepsilon_{tf}$

iii) $\varepsilon_{D_f} \ge \varepsilon_{tf}$

where ε_{tm} is strain at level of extreme tension fiber of concrete section

The strain at the level of bottom of flange (ε_{Df}) is given by

$$\varepsilon_{D_f} = \varepsilon_{cm} \frac{D_f - kd}{kd} \tag{16}$$

Equation (17) shows resultant compressive stress (C_c) in concrete which acts at a distance of $k_2 kd$ from extreme compression fiber.

$$C_c = k_1 f_c b_f kd \tag{17}$$

where k_1 defines the average compressive stress, b_f is the width of flange.

Constants k_1 and k_2 are known as stress block parameters. These stress block parameters can be simply derived from the stress-strain curve by converting it to an equivalent rectangular stress block [2] as

$$k_1 = \frac{\int_0^{\varepsilon_{cm}} \sigma_c d\varepsilon_c}{f_c \varepsilon_{cm}} \tag{18}$$

$$k_2 = 1 - \frac{\int_0^{\varepsilon_{cm}} \varepsilon_c \sigma_c d\varepsilon_c}{\varepsilon_{cm} \int_0^{\varepsilon_{cm}} \sigma_c d\varepsilon_c} \tag{19}$$

Fig. 3 (a), (b), (c) and (d) shows the stress variations for $kd \le D_f$. Stress block parameters k_{3w}, k_{3f}, k_{4w}, and k_{4f}, can be derived by converting the stress-strain curve of concrete in tension into an equivalent rectangular stress block. Equations 20-23 shows these stress block parameters.

For $\varepsilon_{tm} \le \varepsilon_{tp}$

$$k_{3w} = \frac{\int_0^{\varepsilon_{tm}} E_c \varepsilon_c d\varepsilon_c}{f_t \varepsilon_{tm}} \tag{20}$$

$$k_{4w} = 1 - \frac{\int_0^{\varepsilon_{tm}} E_c \varepsilon_c^2 d\varepsilon_c}{\varepsilon_{tm} \int_0^{\varepsilon_{tm}} E_c \varepsilon_c d\varepsilon_c} \tag{21}$$

$$k_{3f} = \frac{\int_0^{\varepsilon_{Df}} E_c \varepsilon_c d\varepsilon_c}{f_t \varepsilon_{tm}} \tag{22}$$

$$k_{4f} = 1 - \frac{\int_0^{\varepsilon_{Df}} E_c \varepsilon_c^2 d\varepsilon_c}{\varepsilon_{tm} \int_0^{\varepsilon_{Df}} E_c \varepsilon_c d\varepsilon_c} \tag{23}$$

The resultant stress for web component which acts at a distance of k_{4w} (D-kd) from extreme tension fiber is given by

$$C_{tw} = k_{3w} f_t b_w (D - kd) \tag{24}$$

where k_{3w} is the average tensile stress for web portion and b_w is width of the web

The resultant stress for the flange component which acts at a distance of k_{4f}(D-kd) from extreme tension fiber is given by

$$C_{tf} = k_{3f} f_t (b_f - b_w)(D - kd) \tag{25}$$

Calculation of kd and moment (M) is as given by equation 26 and 27.

$$kd = \frac{k_{3w} f_t w_w D + k_{3f} f_t (w_f - w_w) D + f_{st} A_{st} - f_{sc} A_{sc}}{k_1 f_c w_f + k_{3w} f_t w_w + k_{3f} f_t (w_f - w_w)} \tag{26}$$

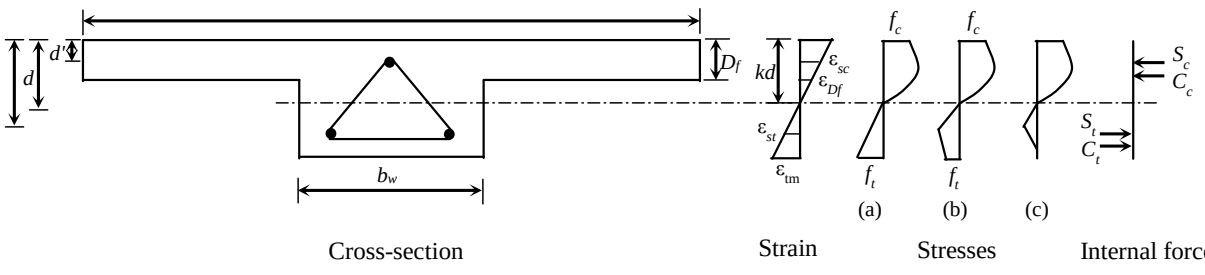

Figure 4 Cross-section of T-beam showing variation of strains and stresses for neutral axis outside the flange

Proc. of the Third Intl. Conf. on Advances in Civil, Structural and Construction Engineering - CSCE 2015

ISBN: 978-1-63248-079-8 doi: 10.15224/ 978-1-63248-079-8-50

$$\begin{aligned} M &= C_c\left(kd - k_2 kd\right) + S_c\left(kd - dd_t\right) \\ &+ C_{tw}\left[\left(D - kd\right) - k_{4w}\left(D - kd\right)\right] \\ &+ C_{tf}\left[\left(D - kd\right) - k_{4f}\left(D - kd\right)\right] \\ &+ S_t\left(d - kd\right) \end{aligned} \quad (27)$$

B. Neutral axis outside the flange $\left(kd > D_f\right)$

When the neutral axis lies outside the flange, a part of web and whole flange will be in compression. Fig. 4 shows the variation of stresses when the neutral axis lies outside the flange The cases considered are as shown in Fig. 4 (a), (b), and (c) and listed below

a) $\varepsilon_{tm} \le \varepsilon_{tp}$

b) $\varepsilon_{tp} < \varepsilon_{tm} < \varepsilon_{tf}$

c) $\varepsilon_{tm} \ge \varepsilon_{tf}$

Strain at the level of bottom of flange is given by

$$\varepsilon_{D_f} = \varepsilon_{cm}\frac{kd - D_f}{kd} \quad (28)$$

The resultant compressive stress is divided into a web component and a flange component. The resultant stress for web component which acts at a distance of $k_{2w}kd$ from extreme compression fiber is given by

$$C_{cw} = k_{1w} f_c b_f kd \quad (29)$$

where k_{1w} is the average compressive stress for web portion and b_f is width of the flange

The resultant stress for the flange component which acts at a distance of $k_{2f}kd$ from extreme tension fiber is given by

$$C_{cf} = k_{1f} f_c\left(b_f - b_w\right)D_f \quad (32)$$

Stress block parameters, resultant tensile stresses, and conditions of force and moment equilibrium for strain at the level of peak tensile stress (ε_{tp}) is greater than or equal to strain in at the level of extreme tension fiber (ε_{tm}) can be given by equations 33-43

For $\varepsilon_{tm} \le \varepsilon_{tp}$

$$k_{1w} = \frac{\int_0^{\varepsilon_{cm}} \sigma_c d\varepsilon_c}{f_c \varepsilon_{cm}} \quad (33)$$

$$k_{2w} = 1 - \frac{\int_0^{\varepsilon_{cm}} \sigma_c \varepsilon_c}{\varepsilon_{cm}\int_0^{\varepsilon_{cm}} \sigma_c d\varepsilon_c} \quad (34)$$

$$k_{1f} = \frac{\int_{\varepsilon_{D_f}}^{\varepsilon_{cm}} \sigma_c d\varepsilon_c}{f_c \varepsilon_{cm}} \quad (35)$$

$$k_{2f} = 1 - \frac{\int_{\varepsilon_{D_f}}^{\varepsilon_{cm}} \sigma_c \varepsilon_c}{\varepsilon_{cm}\int_{\varepsilon_{D_f}}^{\varepsilon_{cm}} \sigma_c d\varepsilon_c} \quad (36)$$

$$k_3 = \frac{\int_0^{\varepsilon_{tm}} E_c \varepsilon_c d\varepsilon_c}{f_t \varepsilon_{tm}} \quad (37)$$

$$k_4 = 1 - \frac{\int_0^{\varepsilon_{tm}} E_c \varepsilon_c^2 d\varepsilon_c}{\varepsilon_{tm}\int_0^{\varepsilon_{tm}} E_c \varepsilon_c d\varepsilon_c} \quad (38)$$

$$C_{cw} = k_{1w} f_c w_w kd \quad (39)$$

$$C_{cf} = k_{1f} f_c\left(w_f - w_w\right)kd \quad (40)$$

$$C_t = k_3 f_t w_w\left(D - kd\right) \quad (41)$$

$$kd = \frac{k_3 f_t w_w D + f_{st}A_{st} - f_{sc}A_{sc}}{k_{1w} f_c w_w + k_{1f} f_c\left(w_f - w_w\right) + k_3 f_t w_w} \quad (42)$$

$$\begin{aligned} M &= C_{cw}\left(kd - k_{2w}kd\right) \\ &+ C_{cf}\left(kd - k_{2f}kd\right) + S_c\left(kd - dd_t\right) \\ &+ C_t\left[\left(D - kd\right) - k_3\left(D - kd\right)\right] + S_t\left(d - kd\right) \end{aligned} \quad (43)$$

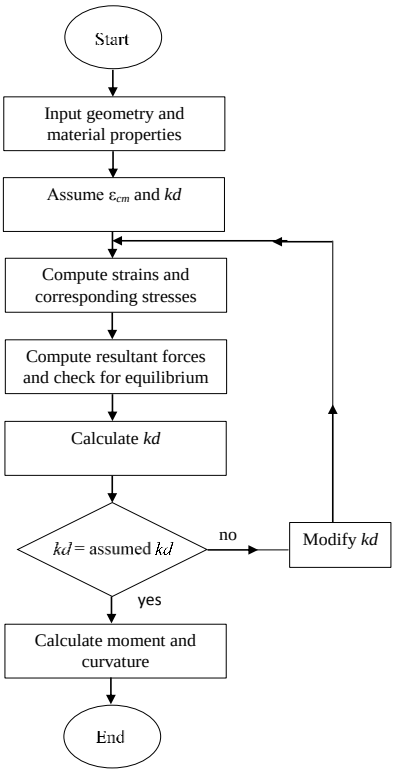

Figure 5 Algorithm showing step by step procedure to generate moment-curvature relation

Proc. of the Third Intl. Conf. on Advances in Civil, Structural and Construction Engineering - CSCE 2015

ISBN: 978-1-63248-079-8 doi: 10.15224/ 978-1-63248-079-8-50

An algorithm has been written in MATLAB to generate the moment-curvature relation for a reinforced concrete T-beam section as shown in Fig. 5 considering all the cases mentioned above. Finally, curvature is calculated as

$$\varphi = \frac{\varepsilon_{cm}}{kd} \tag{44}$$

III. Experimental data

A. *Details of the test specimens*

Experiments conducted at Structural Engineering Laboratory, IIT Madras on three simply supported RC T-beams subjected to symmetric two point loading simulating pure bending. Fig. 6 shows the photograph of one of the test specimens. The beams were tested under two point loads. Effective span (l) of the beam is 2750 mm. The load was applied at a distance of l/4 from both the ends, with the help of hydraulic jack. Deflections were recorded using LVDT (Linear variable displacement transducer) positioned at the midspan as well as the two loads points. The geometrical and material properties of the test specimens are tabulated in Table I and Table II. The yield strength of steel is 500N/mm^2. The beams were casted using ready mixed concrete and cured for 28 days.

TABLE I. GEOMETRIC PROPERTIES OF TEST SPECIMENS

Beam.	b_f (mm)	D (mm)	D_f (mm)	b_w (mm)
1S5R12	770	174	50	230
1S7R10	770	194	70	230
1S7R12	770	194	70	230

TABLE II. MATERIAL PROPERTIES OF TEST SPECIMENS

Beam.	f_c (MPa)	A_{st} (mm^2)	A_{sc} (mm^2)
1S5R12	25	3Y12	1Y10
1S7R10	25	2Y10	1Y10
1S7R12	25	3Y12	1Y10

Figure. 6 Photograph of the experimental setup

Tensile reinforcement and depth of flange are the two parameters considered in this experimental study. Specimen 1S7R10 has lower reinforcement compared to the other two specimens (1S5R12 and 1S7R12) to study the effect of tensile reinforcement on moment capacity of the beam section. Keeping the tensile reinforcement constant, specimens 1S5R12 and 1S7R12 are studied to understand the influence of depth of flange.

B. *Generation of moment-curvature relation from experimental load-deflection data*

The deflection profile between the loading points takes shape of an arc of a circle with radius R and a constant drift from central line as shown in Fig. 7 in a pure bending region. Using theory of simple bending, the curvature can be calculated from the deflection data obtained from the experiments as explained below.

Curvature of the beam section given by

$$\varphi = \frac{1}{R} \tag{45}$$

From Fig. 7,

$$OC' = OD' = OE' = R \tag{46}$$

where R is radius of the circle.

Using Pythagoras theorem,

$$OC'^2 + CD'^2 = OD'^2 \tag{47}$$

$$OC' = OM - C'M = R - \left(\Delta_{mid} - \Delta_L\right) = R - y \tag{48}$$

Substituting this value in (47) and solving,

$$R^2 - 2Ry + y^2 + l^2/4 = R^2 \tag{49}$$

$$R = \frac{y^2 + l^2/4}{2y} \tag{50}$$

From (45), we get

$$\varphi = \frac{1}{R} = \frac{2y}{y^2 + l^2/4} \tag{51}$$

$$y = \Delta_{mid} - \Delta_L \tag{52}$$

Substituting (52) in (51), curvature for a given cross-section of a beam from the experimental load-deflection data can be calculated.

Moment at mid-span of the simply supported beam (determinate structure) can be calculated as

$$M = \frac{PL}{8} \tag{53}$$

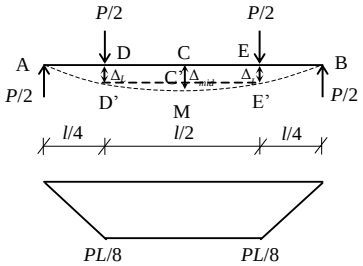

Bending moment diagram

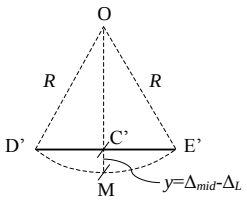

Span showing an arc of circle between the load points

Figure 7 Deflection profile and bending moment diagram for the beam

Proc. of the Third Intl. Conf. on Advances in Civil, Structural and Construction Engineering - CSCE 2015

ISBN: 978-1-63248-079-8 doi: 10.15224/ 978-1-63248-079-8-50

IV. Validation of the algorithm with the experimental data

Moment-curvature curves obtained from the numerical algorithm are compared with that generated from the experiment. The comparison between the numerical and the experimental results are presented in Fig. 8 to Fig. 12

It can be inferred from the comparisons shown in the Fig. 8 to 12 that, the results generated using the proposed numerical algorithm are in good agreement with that obtained from the experiments. Fig. 11 shows that increase in the depth of flange increases the moment capacity of the section as expected. Similarly, moment capacity is higher for the higher percentage of steel as seen in Fig.12.

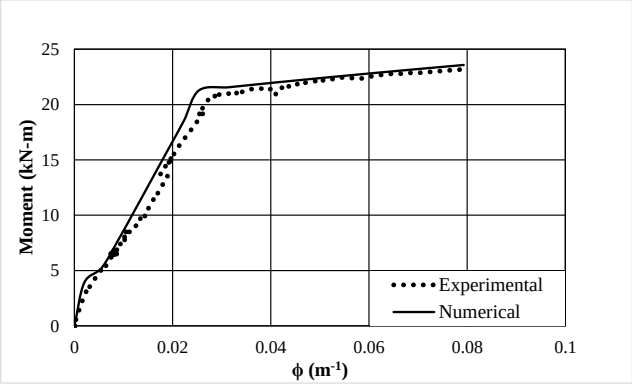

Figure 8 Comparison of numerical and experimental moment-curvature curve for 1S5R12

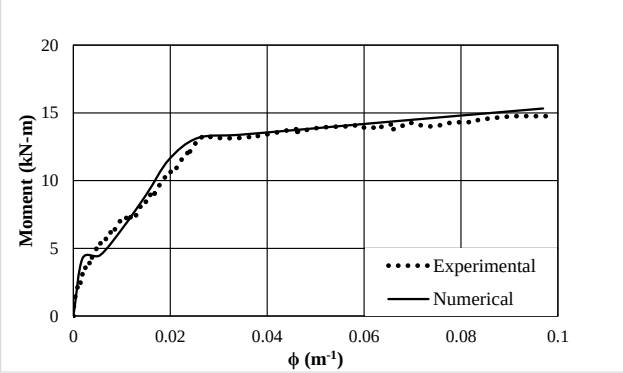

Figure 9 Comparison of numerical and experimental moment-curvature curve for 1S7R10

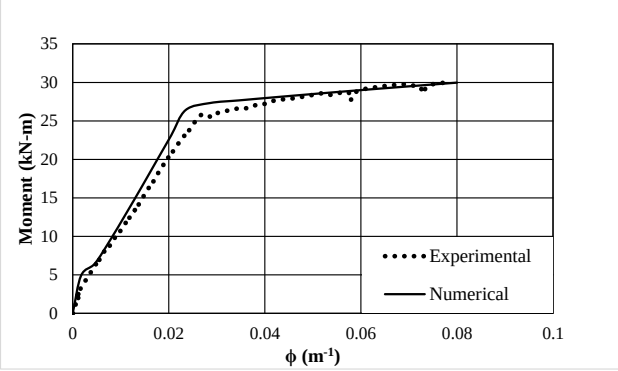

Figure 10 Comparison of numerical and experimental moment-curvature curve for 1S7R12

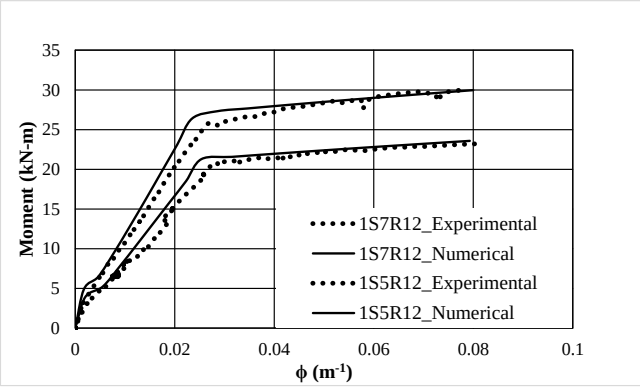

Figure 11 Comparision of moment-curvature graphs for variation in depth of flange

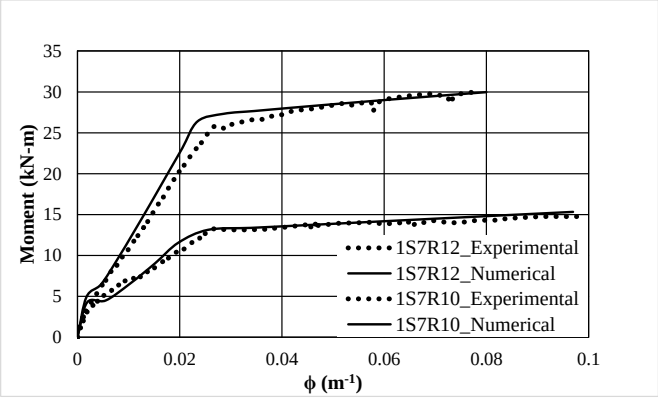

Figure 12 Comparision of moment-curvature graphs for variation in tensile reinforcement

Conclusions

The numerical algorithm developed is simple and efficient, and predicts the moment-curvature relation quite accurately. It can also be conveniently invoked as an input in the numerical analysis, to predict the nonlinear load-deflection behaviour as well as in studies related to probabilistic analysis and optimization, where the nonlinear analysis has to be repeatedly executed.

The results show that the variables considered in the study i.e. depth of flange and tensile reinforcement contributes significantly to the moment capacity of the section.

Acknowledgement

Authors acknowledge Structural Engineering Laboratory, Department of Civil Engineering, IIT Madras for providing facilities to conduct experimental works.

References

[1] Shariff, M. N. (2013). Nonlinear analysis of RC beams, frames and grids, Master of Science thesis, Dept. of Civil Engineering, Indian Institute of Technology Madras, Chennai, India.

[2] Bazant, P., and Oh, B. (1984). Deformation of progressively cracking reinforced concrete beams, ACI Structural Journal, 81, 268-278.

[3] Carreira, D.J., and Chu, K.-H. (1985). Stress-strain relationship for plain concrete in compression", ACI Structural Journal, 82, 797-804.

[4] Carreira, D.J. and Chu, K.-H. (1986). Stress-strain relationship for reinforced concrete in tension. ACI Journal Proceedings, 83(1), 21-28.

ISBN: 978-1-63248-079-8 doi: 10.15224/ 978-1-63248-079-8-50

[5] Prakhya, G.K.V., and Morley, C.T. (1990) Tension-stiffening and moment-curvature relations of reinforced concrete elements. ACI Structural Journal, 87, 567-605.

[6] Pillai, S.U., and Menon, D. Reinforced Concrete Design, Third Edition, Tata McGraw Hill, New Delhi, 2009.

[7] Desayi, P., and Krishnan, S., (1964) Equation for the stress-strain curve of concrete, ACI Structural Journal, 61, 345-350.

[8] Alwis, W.A.M. (1990) Trilinear moment curvature relationship for reinforced concrete beams. ACI Structural Journal, 87, 276-283.

[9] ACI Committee 209, "Prediction of Creep, Shrinkage, and Temperature Effects in Concrete Structures", ACI 209R-92 (Reapproved 1997), American concrete institute, USA.

[10] Belarbi, A., and Hsu, T.T.C. (1994) Constitutive laws of concrete in tension and reinforcing bars stiffened by concrete, ACI Structural Journal, 91, 465-474